



Kent Academic Repository

Mendez Torrecillas, Carlota, Halbert, Gavin W. and Lamprou, Dimitrios A. (2017) *A novel methodology to study polymodal particle size distributions produced during continuous wet granulation*. International Journal of Pharmaceutics 519 (1-2). pp. 230-239. ISSN 0378-5173.

Downloaded from

<https://kar.kent.ac.uk/59858/> The University of Kent's Academic Repository KAR

The version of record is available from

<https://doi.org/10.1016/j.ijpharm.2017.01.023>

This document version

Author's Accepted Manuscript

DOI for this version

Licence for this version

CC BY-NC-ND (Attribution-NonCommercial-NoDerivatives)

Additional information

Versions of research works

Versions of Record

If this version is the version of record, it is the same as the published version available on the publisher's web site. Cite as the published version.

Author Accepted Manuscripts

If this document is identified as the Author Accepted Manuscript it is the version after peer review but before type setting, copy editing or publisher branding. Cite as Surname, Initial. (Year) 'Title of article'. To be published in *Title of Journal*, Volume and issue numbers [peer-reviewed accepted version]. Available at: DOI or URL (Accessed: date).

Enquiries

If you have questions about this document contact ResearchSupport@kent.ac.uk. Please include the URL of the record in KAR. If you believe that your, or a third party's rights have been compromised through this document please see our [Take Down policy](https://www.kent.ac.uk/guides/kar-the-kent-academic-repository#policies) (available from <https://www.kent.ac.uk/guides/kar-the-kent-academic-repository#policies>).

1 **A novel methodology to study polymodal particle size distributions produced during**
2 **continuous wet granulation**

3

4 **Carlota Mendez Torrecillas^{1,2*}, Gavin W. Halbert^{1,2**}, Dimitrios A. Lamprou^{2,3*},**

5

6 ¹ EPSRC Centre for Innovative Manufacturing in Continuous Manufacturing and
7 Crystallisation (CMAC), University of Strathclyde, Technology and Innovation Centre, 99
8 George Street, G1 1RD Glasgow, United Kingdom.

9 ² Strathclyde Institute of Pharmacy and Biomedical Sciences (SIPBS), University of
10 Strathclyde, 161 Cathedral Street, G4 0RE Glasgow, United Kingdom.

11 ³ Medway School of Pharmacy, University of Kent, Medway Campus, Anson Building, Central
12 Avenue, Chatham Maritime, Chatham, Kent, ME4 4TB, United Kingdom.

13 * Corresponding Authors. E-mail address: carlota.mendez@strath.ac.uk and
14 D.Lamprou@kent.ac.uk.

15 Tel.: +44(0) 163 420 2947.

16 ** Funded by Cancer Research UK

17

18 **ABSTRACT**

19 It is important during powder granulation to obtain particles of a homogeneous size especially
20 in critical situations such as pharmaceutical manufacture. To date, homogeneity of particle size
21 distribution has been defined by the use of the d_{50} combined with the span of the particle size
22 distribution, which has been found ineffective for polymodal particle size distributions. This
23 work focuses on demonstrating the limitations of the span parameter to quantify homogeneity
24 and proposes a novel improved metric based on the transformation of a typical particle size
25 distribution curve into a homogeneity factor which can vary from 0 to 100%. The potential of
26 this method as a characterisation tool has been demonstrated through its application to the
27 production of granules using two different materials. The workspace of an 11 mm twin screw
28 granulator was defined for two common excipients (α -lactose monohydrate and
29 microcrystalline cellulose). Homogeneity of the obtained granules varied dramatically from 0
30 to 95 % in the same workspace, allowing identification of critical process parameters (e.g. feed
31 rate, liquid/solid ratio, torque velocities). In addition it defined the operational conditions
32 required to produce the most homogeneous product within the range 5 μm – 2.2 mm from both
33 materials.

34 **Keywords:** Twin screw granulation; particle size distribution; homogeneity factor; quality by
35 design; granules.

36

37

38

39

40

41 **Abbreviations:**

- 42 A_0 Area corresponding to the equivalent minimum homogeneity of PSD
- 43 A_{100} Area corresponding to the equivalent maximum homogeneity of PSD
- 44 A_{PSD} Area corresponding to the PSD
- 45 DoE Design of experiments
- 46 d_x Intercept x of the cumulative volume
- 47 d Diameter
- 48 FH Homogeneity factor
- 49 k_1 Sorting factor parameter
- 50 k_2 Sorting factor parameter
- 51 L/S Liquid/Solid ratio
- 52 μ Mean value
- 53 n_{interv} Number of intervals
- 54 p Percentage of the value of the population
- 55 PSD Particle Size Distribution
- 56 QbD Quality by Design
- 57 q_x Density distribution
- 58 Q_x Cumulative distribution
- 59 s Sorting factor
- 60 VMD Volume mean diameter

- 61 TSG Twin-Screw Granulator
- 62 $w(d)$ Weight distribution
- 63 w_{PSD} Weight distribution corresponding to the particle size distribution
- 64 w_0 Weight distribution corresponding to the equivalent minimum homogeneity of PSD
- 65 w_{100} Weight distribution corresponding to the equivalent maximum homogeneity of PSD
- 66 x_m Particle size
- 67 x_{m_0} Particle size of the first value
- 68 $x_{m_{max}}$ Particle size of the maximum peak
- 69

70 **1. INTRODUCTION**

71 Wet granulation is a common industrial unit operation in the pharmaceutical industry for
72 particle size enlargement. Although this operation has been traditionally performed in batch,
73 it could be effectively achieved in a continuous mode using a Twin-Screw Granulator (TSG).
74 The key advantages of this technology over batch granulation are shorter residence times,
75 greater flexibility in granule properties and the ability to vary the required throughput. The
76 understanding of wet granulation has achieved notable advances in the past twenty-five years,
77 since the macroscopic research of granulation was replaced by a microscopic study of the
78 variables ((Ennis and Litster, 1997; Ennis, 1991; Parikh, 2005)).

79 In contrast to batch equipment traditionally used in wet granulation, TSG has been applied by
80 the pharmaceutical industry as a useful continuous operation granulation technique (Keleb et
81 al., 2002; Van Melkebeke et al., 2008), which due to the flexibility offered by the equipment
82 is easier to design and scale up. Multiple working environments are enabled by the possibility
83 of changing different sections of the screw assembly, feed port locations, different segment
84 geometry's or the option of working with a wide range of conditions such as feed rate or
85 liquid/solid ratio (Dhenge et al., 2011; Djuric and Kleinebudde, 2008; Vercruysse et al., 2012).
86 Vercruysse (Vercruysse et al., 2013), for example confirmed the successful production of
87 granules by TSG processes within the specifications defined for the equivalent batch fluid bed
88 granulation process. Furthermore, this system was able to manufacture simplified formulations
89 containing high drug loads of up to 90% (Meier et al., 2015). On the contrary, other cases
90 where there is a lack of specific tools to study the operational parameters were driven to
91 situations where the implementation of TSG was not justified compared to batch systems (Lee
92 et al., 2013).

93 One of the main explanations is that the variation in the conditions produces many different
94 Particle Size Distributions (PSD) for which the curves differ from the desired unimodal shape
95 (Yu et al., 2014) achieved during standard batch granulation processes. The appearance of
96 polymodal distributions is especially prevalent during research into the effects that the
97 parameters have on granule properties. Particle size distributions vary from unimodal to
98 polymodal depending on the analysed value or position of the variable. That is especially
99 remarkable, in the different studies about the influence of the main parameters such as
100 liquid/solid ratio (L/S) or screw elements (Dhenge et al., 2012; El Hagrasy et al., 2013; Sayin
101 et al., 2015).

102 The evaluation of the granulation process requires knowledge of the variance of the granules'
103 properties as function of the process parameters, and, the establishment of the variation using
104 general terms such as volume, strength, and friability. The study of these terms gives important
105 information allowing process control, as well as establishment of the acceptable limits of the
106 working conditions. However, although terms such as friability or flowability can be expressed
107 as a single value, particle size distribution is frequently expressed as a curve, which does not
108 allow its direct examination as a quality attribute or a process control variable. A quality
109 attribute should be within an appropriate limit, range, or distribution to ensure the desired
110 product quality (ICH Q8 (R2), 2009).

111 The separation of a particulate sample into discrete size classes has been traditionally
112 performed representing the type of quantity in the abscissa and the measure of the quantity in
113 the ordinate. The measurement of the quantity is made through the relative amount of particles
114 measured within a specific size interval and it is called density distribution (q_x). This term is
115 the first derivative of the cumulative distribution (Q_x) against particle size (Leschonski, 1984).
116 The subscript x represents the type of quantity where the possible types are number, length,
117 area, volume or mass. In pharmaceutical sciences, the type of quantity chosen is frequently the

118 volume, due to the importance of the relationship between drug delivery and volume (Müllertz
119 et al., 2016).

120 Frequently, the volume particle size distributions are characterised by d_{10} , d_{50} and d_{90} which are
121 calculated through the intercepts for 10, 50 and 90 % of the cumulative volume (ISO, 2014).
122 These terms can be gathered if they are transformed to the span $((d_{90} - d_{10})/d_{50})$ (Chitu et al.,
123 2011; El Hagrasy et al., 2013), with particle size distributions considered more homogeneous
124 the closer this value is to zero. This analysis is only acceptable when the particle size
125 distribution is lognormal, but will introduce a considerable error when the distributions show
126 more than one peak and the peaks are located around the mean diameter. For instance, Figure
127 1 shows two particle size distributions which have two different shapes but very close span
128 values. The first shape (Figure 1a) could be considered to be a common lognormal distribution
129 where all the values are around the main peak. However, the second shape (Figure 1b) displays
130 three peaks of different population densities which indicates that three main types of granules
131 exist in the sample. Nevertheless, the difference between spans of those distributions is less
132 than 2%, and therefore both distributions would be comparable in terms of homogeneity even
133 if they are clearly different in the number of peaks.

134 In sedimentology an alternative method has been applied to transform the normal distribution
135 for unimodal and bimodal distributions known as the hyperbolic tangent technique (tanh
136 method), which has been used traditionally for dealing with travelling waves and to study
137 evolution equations (Malfliet, 2004). It was successfully applied by Passe (Passe, 1997) in
138 order to transform a grain distribution into a mathematical expression. Due to the fact that the
139 graphical result of the integral of a normal distribution presents an analogous shape to the
140 hyperbolic tangent function; the cumulative expression can be mathematically described by
141 Eq. 1.

$$w(d) = \frac{p}{2} - \left(\frac{p}{2}\right) * \tanh(\log(\mu) - \log(d) * s) \quad \text{Eq. 1}$$

142 Where w is the weight, μ is the mean value of the particle size, d is the variable particle size, p
143 is the value of the population of the different peaks in percentage which is equal to 100% for
144 unimodal distributions and s is a sorting factor which is given as $1/(\log d_{75} - \log d_{25})$ (Passe,
145 1997).
146

147 This technique for transforming curves into mathematical expressions can be used as an
148 effective way to smooth distribution curves due to the variation of the slope depending on the
149 number of peaks. For example, three different particle size distributions have been transformed
150 through this method in Figure 2 representing the weight against the logarithm of the particle
151 size. The first PSD (Figure 2a) can be considered as a mono-modal distribution and its
152 equivalent weight distribution is a straight line which slopes up at the greatest rate. The second
153 PSD (Figure 2b) corresponds to a bimodal distribution and its weight distribution shows an
154 important decrease of the slope of the curve compared to Figure 2a. The third PSD (Figure 2c)
155 represents a polymodal distribution with three clear peaks in which the slope of the
156 corresponding weight distribution curve has decreased even more dramatically with respect to
157 Figure 2a. Therefore, from Figure 2 it can be concluded that the decreasing slope of the curves
158 represents the decrease in homogeneity of distribution as well as the increase in the number of
159 peaks of the distribution.

160 The direct relationship between the slope of the weight distribution curve and the shape of the
161 particle size distribution shows an enormous potential as a characterisation tool. The area under
162 the resultant curve can be calculated through integration and it will be proportional to the slope
163 of the curve. The homogeneity can be measured through this method and transformed into a
164 percentage, unimodal PSDs will be associated with larger areas and greater homogeneity
165 percentages.

166 Transforming PSDs into a homogeneity factor (FH) allows the analysis of the influence of
167 operational parameters on the system. In addition, workspaces can be created and the system
168 can be easily optimised after obtaining the regions where the production of granules is
169 homogeneous.

170 Further potential advantages of homogeneity values calculated from particle size distributions
171 are related to its potential to be used as a characterisation tool for Quality by Design (QbD)
172 which is recommended for adoption by the pharmaceutical industry (Seem et al., 2015). This
173 approach ought to be accomplished with a systematic scientific risk-based methodology,
174 therefore a tool for characterising granule homogeneity would help to provide a greater
175 understanding of the underlying process mechanisms. In addition, it will improve the control
176 during granule manufacture as well as being a useful complement to other granule properties
177 such as flowability or strength in the optimisation of tableting and associated processes.
178 Besides, the possibility of defining a desired diameter operating point and controlling the
179 homogeneity around that point allows identification of when the process is within product
180 specifications. This advantage could be used in the comparison of different batches and
181 technologies both research and industrial scale.

182 Due to the possible advantages of quantifying a PSD's homogeneity with a single numerical
183 parameter, the aims of this study were to propose a methodology capable of achieving this.
184 The method developed can transform any PSD into a weight distribution through the hyperbolic
185 tangent method and calculate a homogeneity percentage. Furthermore, this method was
186 mathematically validated through the study of the response to simulated scenarios of particle
187 size distributions and empirically demonstrated through the application to two different
188 materials (α -Lactose monohydrate and microcrystalline cellulose) and its potential as
189 characterisation tool was assessed by determining the most critical process parameters for both
190 systems.

191 **2. MATERIALS AND METHODS**

192 **2.1. Materials**

193 α -Lactose monohydrate (PubChem CID: 24896349) with 99% total lactose basis (GC) (Sigma-
194 Aldrich Company Ltd., Dorset, England) and microcrystalline cellulose (PubChem CID:
195 :16211032) with average particle size 50 μm (Fisher Scientific UK Ltd, Loughborough,
196 Leicestershire, United Kingdom) were used as excipients to validate the method. Distilled
197 water (EMD Millipore™ Pure Water Reservoirs, Millipore SAS, Mosheim, France) was added
198 as granulation liquid.

199 **2.2 Granulation experiments**

200 In order to produce granules, a Thermofisher Pharma 11mm Twin Screw Granulator (Process
201 11, 40:1 L/D, Thermo Fisher Scientific, Karlsruhe, Germany) operating within the range of 50-
202 125 rpm in combination with a gravimetric feeder (Brabender Gravimetric feeder DDW-MT,
203 Brabender Technologie Gmbh & Co. Kg Duisburg, Germany) was employed to feed excipients
204 at a rate of 0.05-0.35 kg h^{-1} . Distilled water was fed to the system through a syringe pump
205 (Harvard Syringe Pump, Harvard Apparatus UK, Cambridge, UK) in order to produce
206 liquid/solid ratios from 0.05 to 0.2 for α -Lactose monohydrate, and 1 to 1.8 for microcrystalline
207 cellulose. The upper and lower limits of granule production ratios were chosen since below the
208 lower limit, the product obtained at these torque velocities was a powder and above the upper
209 limit the product was a wet mass. The design of experiments and following analysis was done
210 through the use of the commercial software Modde 10.1. The chosen model design used to
211 select the experimental setup and to study the relationship between variables was an Onion D-
212 Optimal model with two layers which was fitted afterwards with PLS-2PLS regression analysis
213 (MKS Data Analytics Solutions, Malmö, Sweden). Figure 3 displays the design of experiments
214 for both materials: α -Lactose monohydrate (Figure 3a) and for microcrystalline cellulose

215 (Figure 3b). The screw configuration used was 27 conveying elements for each sheet, chosen
 216 in order to minimise the impact that the different screw elements could have on the granules
 217 (Seem et al., 2015).

218 **2.3 Offline granule size analysis**

219 The analysis of the granule size distribution was performed using the QICPIC/RODOS L with
 220 vibratory feeder VIBRI/L (Sympatec GmbH System-Partikel-Technik, Clausthal-Zellerfeld,
 221 Germany).

222 All the particle size distributions obtained were produced at 0.5 bar of primary pressure to
 223 avoid breakage of the granules during the analysis (MacLeod and Muller, 2012). The disperser
 224 conditions were optimised for each set of granules to obtain the optimal optical concentration.
 225 All the particle size distributions were plotted in logarithmic volume against the particle size.
 226 The volumetric mean diameter (VMD) determined by the system was chosen as mean diameter,
 227 and is been calculated based in the arithmetic mean value.

228 **2.4 Quantification of homogeneity method**

229 To quantify homogeneity PSD curves are smoothed through the hyperbolic tangent method in
 230 order to adapt the data to the mathematical expression in Eq. 2 based in the equation used by
 231 Passe. (Passe, 1997).

$$233 \quad w(xm) = \sum_0^{i=total\ peaks} \left(\frac{p_i}{2} - \frac{p_i}{2} * \tanh(\log(\mu_i) - \log(xm) * s_i) \right)$$

232 Eq. 2

234 Where the subindex i represents the peak number for appearance order, p_i is the value of the
 235 population of the peak in percentage, μ_i is the mean value of the particle size for the peak width,

236 x_m is the size of the particles included in the width of the peak, and s_i is a sorting factor defined
 237 in Eq 3.

238 This mathematical expression depends on the total number of peaks and a specific expression
 239 needs to be developed for each peak. The peaks are local maxima of the particle size
 240 distribution. The local maximum is located as the data point which is larger than its two
 241 neighbouring points, in those cases that the top of the peak is flat, the point considered is the
 242 first to appear (The MathWorks Inc, 2013). After locating the peaks, their amplitude was
 243 calculated by means of the integral of the curve formed by the peak.

244 The sorting factors for each PSD curve are calculated using Eq 3 were d_{25} and d_{75} are the
 245 diameter corresponding to the 25% and 75% population weight of each peak. The sorting factor
 246 was adapted from the method presented by Passe (Passe, 1997) through the introduction of the
 247 terms k_1 and k_2 which were developed in house for the range $5 \mu\text{m} - 2.2 \text{ mm}$. The term k_1
 248 weights the difference between the peak corresponding to maximum value in the density
 249 distribution and the volumetric mean diameter of the particles (Eq. 4). Frequently, the limits
 250 of the ranges of particles sizes distribution are proportional to the size of particle and those
 251 could be different depending on the choice of nest of sieves or the measuring range of the
 252 analytical system. To avoid the effect of these possible discrepancies between the different
 253 methods, the distribution will be normalised when one considers that it is composed of ten
 254 identical intervals. The difference between the maximum peak and the mean diameter will be
 255 measured through the number of intervals between them (Eq. 5).

$$256 \quad s_i = k_1 * \frac{p_i}{\log(d_{75}) - \log(d_{25})} \quad \text{Eq. 3}$$

$$257 \quad k_1 = \exp\left(-\left(\frac{x_{m_{\max \text{ peak}} - d}{k_2}\right)\right) \quad \text{Eq. 4}$$

$$258 \quad k_2 = 10 * \frac{x_{m_{\text{last}}} - x_{m_0}}{n_{\text{interval}}} \quad \text{Eq. 5}$$

259 After the particle size distributions have been smoothed, it is required to achieve the maximum
 260 homogeneity possible, e.g. the distribution obtained when all the granules would have the same
 261 diameter and that coincides with the mean diameter. The maximum homogeneity corresponds
 262 to the best case scenario of a unimodal distribution where the first value which would appear
 263 would be unique and it would produce a single peak. After this equivalent perfect particle size
 264 distribution has been calculated, it is possible to calculate the weight distribution for that case.
 265 The lower limits corresponding to zero homogeneity would be represented by the curves
 266 produced when all the sizes have the same weight inside the distribution. As in the case of the
 267 perfect distribution, the PSD needs to be transformed to worst case scenario, allowing the
 268 weight distribution to be calculated. Figure 4 displays the situation where both maximum and
 269 minimum cases have been transformed into their equivalent distribution. The differences in the
 270 rise of both curves allow to distinguish clearly between them as the curve corresponding to
 271 100% homogeneity has a slope 15 times greater than the curve corresponding to 0%.

272 Once the upper and lower limits have been determined, it is possible to calculate the
 273 homogeneity for any particle size distribution by calculating the area under the curve
 274 corresponding to the PSD and its equivalent best (100% homogeneity) and worst (0%
 275 homogeneity) cases. Figure 5 displays the three areas in different colours. The area
 276 corresponding to 100% homogeneity would be comprised between the solid and dotted black
 277 lines with the PSD area shaded in yellow. Since the particle size distribution is given in
 278 intervals, it was chosen to obtain the area under curve through the trapezoidal rule (Treiman,
 279 2014).

280 The homogeneity factor can then be calculated as percentage using Eq. 6.

$$281 \quad FH (\%) = 100 - 100 * \left(\frac{\int w_{PSD}(\log(xm))dx - \int w_0(\log(xm))dx}{\int w_{100}(\log(xm))dx - \int w_{PSD}(\log(xm))dx} \right) \rightarrow$$

$$282 \quad FH (\%) = 100 - \frac{A_{PSD} - A_0}{A_{100} - A_0} * 100 \quad \text{Eq. 6}$$

283 A summary of the methodology can be found in a flowchart in Figure 6.

284 All the data and analysis processing were performed using the commercial software package
285 Matlab (can be found under the supplemental information) and Statistics Toolbox R2014a (The
286 MathWorks, Inc., Natick, Massachusetts, United States).

287 **2.5 Contour profiles**

288 The results and the effects of the different variables will be presented as contour plots, which
289 are able to show multidimensional interactions between the input variables and process
290 parameters. The contour profiles are a recommended tool to identify the design space of a full
291 workspace (ICH Q8 (R2), 2009). These profiles are built identifying which combinations of
292 the selected parameters produce the same result on the chosen variable and identifying them
293 with the same contour.

294 In this case, for each material analysed four different profiles were produced. Two for each
295 quality attribute (homogeneity factor and volumetric mean diameter) at two different ranges of
296 torque velocity (50-87.5 rpm and 87.5-125 rpm). The chosen process parameters were the mass
297 feed rate of the solid and the liquid/solid ratio (L/S) which is defined as the relationship between
298 the mass feed rate of the solid and the liquid. A schematic of the Design of experiments (DoE)
299 can be found in Figure 3.

300

301

302

303

304

305 **3. RESULTS and DISCUSSION**

306 **3.1 Verification of the methodology**

307 According to Eq.2, the homogeneity factor is sensitive to changes in factors such as the number
308 of the peaks or the width of the distribution. The methodology was verified through comparing
309 the response of different simulated distributions with volumetric mean diameter equal to 1000
310 μm .

311 In the first case (Figure 7a), the effect of modification of the distribution shape was studied
312 through the increase of the standard deviation of the distributions from 0.1 to 0.25. The increase
313 of the standard deviation in a unimodal distribution produced a direct change in the width of
314 the distribution, and as Figure 7a shows that affects directly in the FH. Additionally, Figure 7e
315 shows the trend for greater increases in the standard deviation.

316 In the second case, the effect of introducing a peak (Figure 7b) and three peaks (Figure 7c) can
317 be studied in two different widths. The effect of introducing a new peak produced a fall in the
318 homogeneity as the initial homogeneity is considerably lower than that corresponding to a
319 single peak for both widths. Figure 7f shows the effect of the increase of number of peaks from
320 a unimodal distribution with a standard deviation of 0.25 to five peaks in the same width. As it
321 can see, the addition of peaks produce dramatic falls in the homogeneity.

322 In the last case (Figure d and g), the distance between peaks was studied. The FH is sensitive
323 to the introduction and distance between peaks as the two peaks are far apart showed a lesser
324 degree of homogeneity than when they were closer (Figure 7d).

325 Other factors which will affect the FH are the distance between the volumetric mean diameter
326 and the main peak. Those cases in which the diameter is situated around the main peak will
327 have greater homogeneity than those in which the diameter is more distant.

328 To illustrate this the analysis was applied to three different real samples (see Figure 8) where
329 the homogeneity varied from 0 to 75%. In the first case (Figure 8a) homogeneity is negligible
330 (0%), since the sample has three main classes of particles with two of them with similar
331 intensity in the density curve. However, the volumetric mean diameter (VMD) is skewed by
332 a greater percentage of fines which reduces dramatically the homogeneity. In the second case
333 (Figure 8b), there are again three classes of particles but even if the width is bigger than in the
334 other cases, the mean diameter is placed closer to the middle of the three peaks. Therefore,
335 the sample is more homogeneous than previous case as the VMD is closer to the biggest peak
336 (38.3%). In the third case (Figure 8c), the PSD shape is more similar to a lognormal
337 distribution suggesting the product is more homogeneous (74.8%). In this example, most of the
338 particles have the same diameter. This can be observed from the PSD as well as from the
339 photographs (Figures 8a-c).

340 **3.2 Application of the methodology**

341 The methodology was applied to granules produced in the TSG with two different excipients
342 commonly used in pharmaceutical processing, α -Lactose monohydrate and microcrystalline
343 cellulose, in a wide range of conditions. The results allow understanding of the influence
344 different parameters have on the product homogeneity.

345 The results obtained were presented through contour profiles (Figure 9 and 10). These types of
346 graphs are really effective for summarising entire workspaces. On one hand, once the region
347 of the desired diameter has been located, the operational conditions which produce the most
348 homogeneous granules for that exact diameter can be easily determined.. On the other hand,
349 the contour profiles allow examination of the effects that operational parameters have over the
350 chosen variables. For instance, on a workspace created by changing the value of two
351 parameters, it is possible to identify if the response of the variable has been controlled by only

352 one or both operational parameters. That effect would be noticed since the variable would
353 change linearly and proportionally to the axis of the most relevant parameter. In those cases,
354 that the system would vary depending of both parameters, the response of the variable could
355 adopt different shapes such as slanting or curved lines.

356 As it can be observed in Figure 9, granules of α -Lactose monohydrate were produced using
357 different conditions of liquid/solid (L/S), feed rate and torque velocity. The results show that
358 at low torque velocities (Figures 9a and b), the diameter shows higher dependence on the feed
359 rate than the L/S ratio. The larger granules are produced when the feed rate is reaching the
360 maximum with a high ratio of homogeneity and it can be observed that homogeneity of the
361 process is more influenced by the feed rate than by the L/S ratio.

362 At high torque velocities (Figures 9c and d) homogeneity decreases with respect to the low
363 torque velocities. The maximum homogeneity for this case does not reach 70% and the greater
364 diameter which homogeneity over 50 % is not bigger than 1600 μm . On the contrary to low
365 torque velocities, homogeneity and diameter displayed a nearly equal dependence for both
366 parameters: L/S and feed rate. The production of homogeneous granules is achieved when the
367 feed rate and the L/S ratio are at middle point conditions of the range of operation. At the
368 same time, the diameter increases proportionally to both. For instance, Figure 9d would give
369 a range of operational conditions which produce a target granule diameter. The most adequate
370 parameters to produce a homogeneous product would be found in the Figure 9c, corresponding
371 to a proportion to L/S ratio to Feed rate close to 1.3 to 1.

372 Besides, comparing low torque velocities (Figures 9 a and b) with high torque velocities
373 (Figures c and d), it can be concluded that for α -Lactose monohydrate the degree of filling of
374 the screw is a very important factor. At low torques velocities, high degrees of filling are
375 achieved and the system is more dependant of the amount of powder introduced. At higher

376 velocities, the degree of filling is considerably lower and the system requires a balance between
377 both parameters to obtain a desirable product.

378 Granules of microcrystalline cellulose were produced in an identical manner and the results are
379 presented in Figure 10. Unlike the previous example, the diameter profiles (Figures 10 b and
380 d) show nearly equal dependence to both parameters L/S ratio and feed rate in both cases of
381 torque velocity. However, there is a great difference between the diameters of the particles
382 resulting in granules up to seven times larger than when the system is operated at low torque
383 velocities.

384 On the contrary, homogeneity (Figures 10 a and c) shows greater dependence to the L/S ratio
385 than to feed rate. Furthermore, at L/S ratios above 1.52, the product reaches homogeneities of
386 over 50% in both cases. Comparing the differences between contours profiles at low and high
387 torque velocities indicates that the degree of filling is one of the main factors to take into
388 account in the cellulose microcrystalline example as the low torque velocities show more
389 disturbances than the high torque velocities.

390 In addition to the study individual effects, a comparison between Figures 9 and 10 permits
391 appreciation of the strong behavioural differences between both materials. The growth of both
392 microcrystalline cellulose and α -Lactose monohydrate granules depends dramatically on the
393 L/S ratio, feed rate and torque velocities. Microcrystalline cellulose displays a dramatically
394 greater dependence to the amount of liquid present in the system than α -Lactose monohydrate.
395 This effect agrees with the molecular differences of both materials and the capability of
396 microcrystalline cellulose to physically hold higher amounts of water than α -Lactose
397 monohydrate (Fielden et al., 1988). In addition, these results agree with the outcomes reported
398 by Dhenge *et al.*, where larger granules were also found at the higher L/S ratios (Barrasso et
399 al., 2013; Dhenge et al., 2010). Furthermore, it was described that an increase in powder feed

400 rates reduced the number of peaks in the PSDs (Dhenge et al., 2011), which corresponds with
401 the increase of homogeneity reported in the case of low torque velocities for both materials.
402 Although the most homogeneous product for the studied range were obtained, not all the
403 experimental results can be entirely compared with those presented in the literature due to the
404 crucial role of the screw elements configuration. However, this and published studies all
405 present similar responses to the modifications of the operational parameters as well as similar
406 range of diameters of granules which indicates the validity of this proposed analysis method.
407 Furthermore, this analysis identified the degree of filling as a limiting operational parameter
408 for both materials which will require to be measured quantitatively in further studies of the
409 equipment.

410 **4. CONCLUSIONS**

411 A new methodology for measuring homogeneity of particle size distribution was introduced
412 and validated through its use in two different cases of granulation. The method is able to
413 calculate the homogeneity of PSDs with different shapes allowing easy numerical comparison.
414 The method responded to different modifications such as the addition of peaks, increments on
415 the variation of the distribution or discrepancies between the main diameter and main particle
416 size class. The improvement of this method with respect to the traditional measures such as
417 span was demonstrated through the comparison of PSD curves with different shape but similar
418 span. In addition, the potential of the quantification of homogeneity was demonstrated through
419 the application to simple liquid granulation with two different excipients. In both cases, it was
420 demonstrated that knowing the diameter individually does not give enough information for the
421 ideal conditions to operate or which operational parameters have more influence on the process.
422 Therefore, using homogeneity as a quantified quality attribute leads to a better understanding
423 of powder technology and its possible implementation as characterisation tool in the design
424 and control of wet granulation systems. Future work will involve the study of this tool as
425 process control variable through a sensitivity analysis in an inline process analytical technique.

426

427 **Acknowledgements**

428 The authors would like to thank EPSRC and the Doctoral Training Centre in Continuous
429 Manufacturing and Crystallisation (CMAC) for funding this work. The authors would also like
430 to thank Dr Javier Cardona for corrections in the MatLab code.

- 431 Figure 1. Unimodal (a) and polymodal (b) particle size and cumulative distributions.
- 432 Figure 2. Unimodal (a) and polymodal (b, c) particle size distributions transformed to the
433 equivalent weight distributions (d).
- 434 Figure 3. Design of experiments for α -Lactose monohydrate (a) and cellulose microcrystalline
435 (b).
- 436 Figure 4. Equivalent particle size distributions (a) transformed to weight distributions (b).
- 437 Figure 5. Area under the weight distributions.
- 438 Figure 6. Methodology flowchart.
- 439 Figure 7. Study of the effect of the deviations produced by a change in the amplitude of the
440 peak (a, e), increase of the number of peaks (b, c, f) and distance between the peaks (d, g).
- 441 Figure 8. Granules with homogeneity 0% (a), 38.3% (b) and 74.8% (c).
- 442 Figure 9. Homogeneity and diameter contour profiles for α -Lactose monohydrate: low torque
443 velocities (a, b) and high torque velocities (c, d).
- 444 Figure 10. Homogeneity and diameter contour profiles for cellulose microcrystalline: low
445 torque velocities (a, b) and high torque velocities (c, d).
- 446
- 447

448 **References**

- 449 Barrasso, D., Walia, S., Ramachandran, R., 2013. Multi-component population balance
450 modeling of continuous granulation processes: a parametric study and comparison with
451 experimental trends. *Powder Technology* 241, 85-97.
- 452 Chitu, T.M., Oulahna, D., Hemati, M., 2011. Wet granulation in laboratory-scale high shear
453 mixers: effect of chopper presence, design and impeller speed. *Powder Technology* 206, 34-
454 43.
- 455 Dhenge, R.M., Cartwright, J.J., Doughty, D.G., Hounslow, M.J., Salman, A.D., 2011. Twin
456 screw wet granulation: Effect of powder feed rate. *Advanced Powder Technology* 22, 162-166.
- 457 Dhenge, R.M., Cartwright, J.J., Hounslow, M.J., Salman, A.D., 2012. Twin screw wet
458 granulation: Effects of properties of granulation liquid. *Powder Technology* 229, 126-136.
- 459 Dhenge, R.M., Fyles, R.S., Cartwright, J.J., Doughty, D.G., Hounslow, M.J., Salman, A.D.,
460 2010. Twin screw wet granulation: Granule properties. *Chemical Engineering Journal* 164,
461 322-329.
- 462 Djuric, D., Kleinebudde, P., 2008. Impact of screw elements on continuous granulation with a
463 twin-screw extruder. *Journal of pharmaceutical sciences* 97, 4934-4942.
- 464 El Hagrasy, A., Hennenkamp, J., Burke, M., Cartwright, J., Litster, J., 2013. Twin screw wet
465 granulation: influence of formulation parameters on granule properties and growth behavior.
466 *Powder Technology* 238, 108-115.
- 467 Ennis, B., Litster, J., 1997. Particle size enlargement. *Perry's Chemical Engineers' Handbook*,
468 7th edn, McGraw-Hill, New York, 20-56.
- 469 Ennis, B.J., 1991. On the mechanics of granulation. UMI.
- 470 Fielden, K., Newton, J.M., O'BRIEN, P., Rowe, R.C., 1988. Thermal studies on the interaction
471 of water and microcrystalline cellulose. *Journal of pharmacy and pharmacology* 40, 674-678.
- 472 ICH Q8 (R2), 2009. ICH HARMONISED TRIPARTITE GUIDELINE, Step 4 Version.
- 473 ISO, 2014. Representation of results of particle size analysis Part 2: Calculation of average
474 particle sizes/ diameters and moments from particle size distributions, BS ISO 9276-2:2014.
475 British Standard Institution.
- 476 Keleb, E., Vermeire, A., Vervaet, C., Remon, J.P., 2002. Continuous twin screw extrusion for
477 the wet granulation of lactose. *International journal of pharmaceutics* 239, 69-80.
- 478 Lee, K.T., Ingram, A., Rowson, N.A., 2013. Comparison of granule properties produced using
479 Twin Screw Extruder and High Shear Mixer: A step towards understanding the mechanism of
480 twin screw wet granulation. *Powder Technology* 238, 91-98.

- 481 Leschonski, K., 1984. Representation and evaluation of particle size analysis data. *Particle &*
482 *Particle Systems Characterization* 1, 89-95.
- 483 MacLeod, C.S., Muller, F.L., 2012. On the fracture of pharmaceutical needle-shaped crystals
484 during pressure filtration: case studies and mechanistic understanding. *Organic Process*
485 *Research & Development* 16, 425-434.
- 486 Malfliet, W., 2004. The tanh method: a tool for solving certain classes of nonlinear evolution
487 and wave equations. *Journal of computational and applied mathematics* 164, 529-541.
- 488 Meier, R., Thommes, M., Rasenack, N., Krumme, M., Moll, K.P., Kleinebudde, P., 2015.
489 Simplified formulations with high drug loads for continuous twin-screw granulation.
490 *International Journal of Pharmaceutics* 496, 12-23.
- 491 Müllertz, A., Perrie, Y., Rades, T., 2016. Analytical Techniques in the Pharmaceutical
492 Sciences. *Advances in delivery science and technology*.
- 493 Parikh, D.M., 2005. *Handbook of pharmaceutical granulation technology*. CRC Press.
- 494 Passe, T., 1997. Grain size distribution expressed as tanh-functions. *Sedimentology* 44, 1011-
495 1014.
- 496 Sayin, R., Martinez-Marcos, L., Osorio, J.G., Cruise, P., Jones, I., Halbert, G.W., Lamprou,
497 D.A., Litster, J.D., 2015. Investigation of an 11 mm diameter twin screw granulator: Screw
498 element performance and in-line monitoring via image analysis. *International Journal of*
499 *Pharmaceutics* 496, 24-32.
- 500 Seem, T.C., Rowson, N.A., Ingram, A., Huang, Z., Yu, S., de Matas, M., Gabbott, I., Reynolds,
501 G.K., 2015. Twin screw granulation—A literature review. *Powder Technology* 276, 89-102.
- 502 The MathWorks Inc, 2013. Release, Matlab. Inc., Natick, Massachusetts, United States 488.
- 503 Treiman, J.S., 2014. *Calculus with Vectors*. Springer.
- 504 Van Melkebeke, B., Vervaet, C., Remon, J.P., 2008. Validation of a continuous granulation
505 process using a twin-screw extruder. *International journal of pharmaceutics* 356, 224-230.
- 506 Vercruyssen, J., Córdoba Díaz, D., Peeters, E., Fonteyne, M., Delaet, U., Van Assche, I., De
507 Beer, T., Remon, J.P., Vervaet, C., 2012. Continuous twin screw granulation: Influence of
508 process variables on granule and tablet quality. *European Journal of Pharmaceutics and*
509 *Biopharmaceutics* 82, 205-211.
- 510 Vercruyssen, J., Delaet, U., Van Assche, I., Cappuyns, P., Arata, F., Caporicci, G., De Beer, T.,
511 Remon, J.P., Vervaet, C., 2013. Stability and repeatability of a continuous twin screw
512 granulation and drying system. *European Journal of Pharmaceutics and Biopharmaceutics* 85,
513 1031-1038.

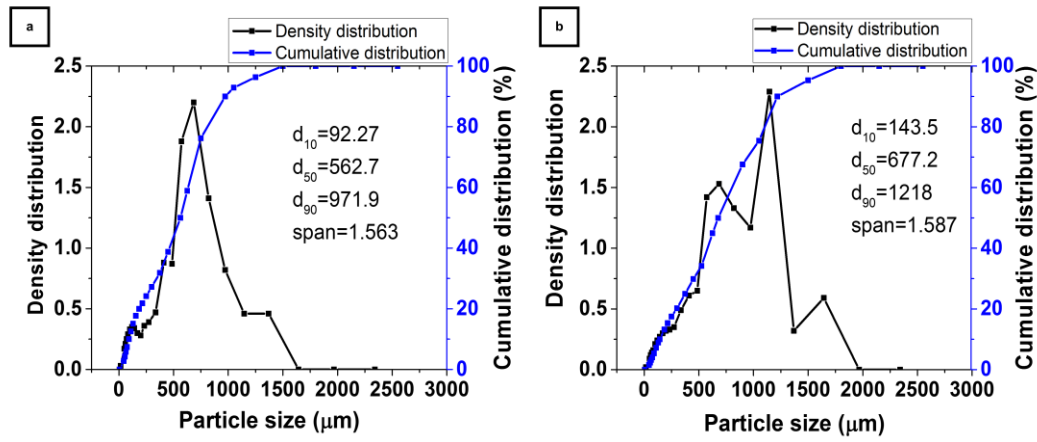
514 Yu, S., Reynolds, G.K., Huang, Z., de Matas, M., Salman, A.D., 2014. Granulation of
515 increasingly hydrophobic formulations using a twin screw granulator. International journal of
516 pharmaceutics 475, 82-96.

517

518

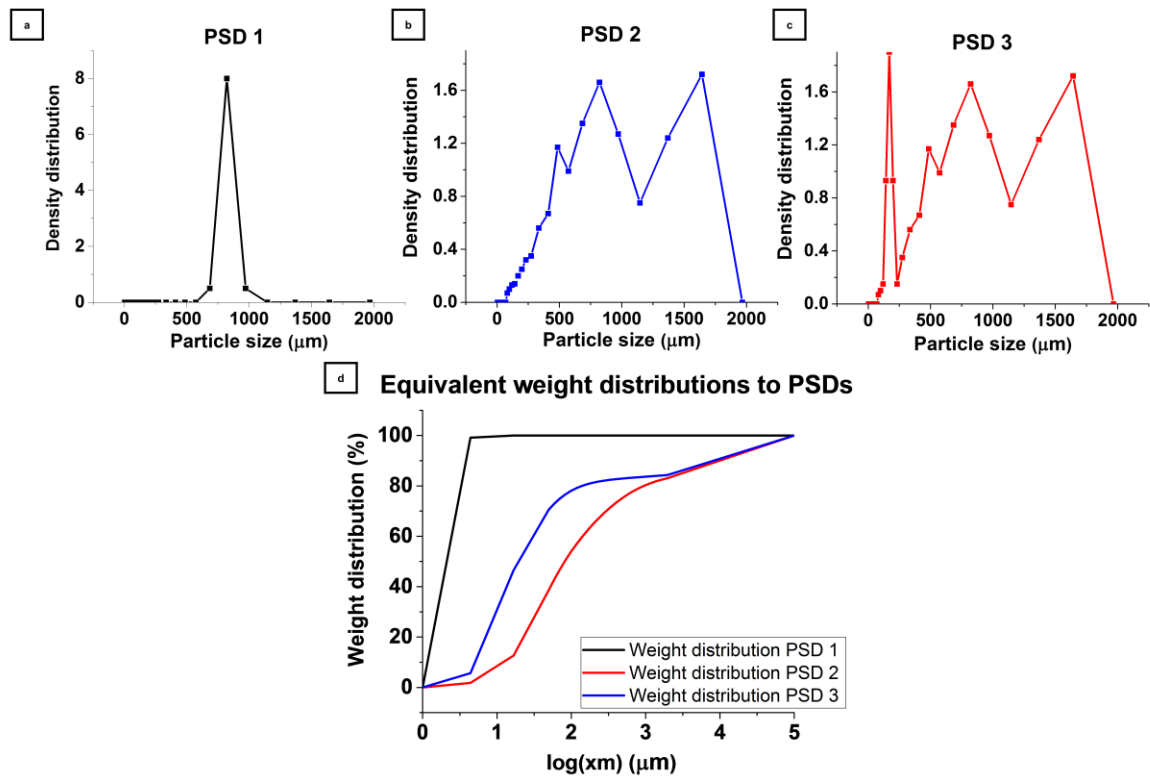
519 Figure 1.

520



521

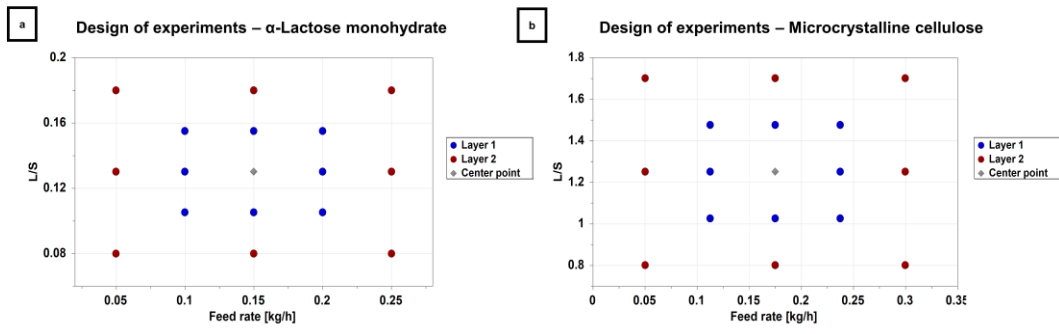
522 Figure 2.



523

524

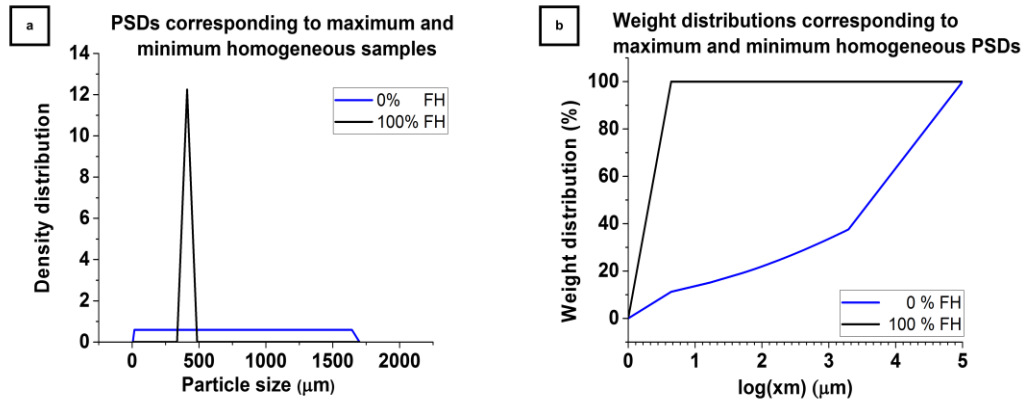
525 Figure 3.



526

527

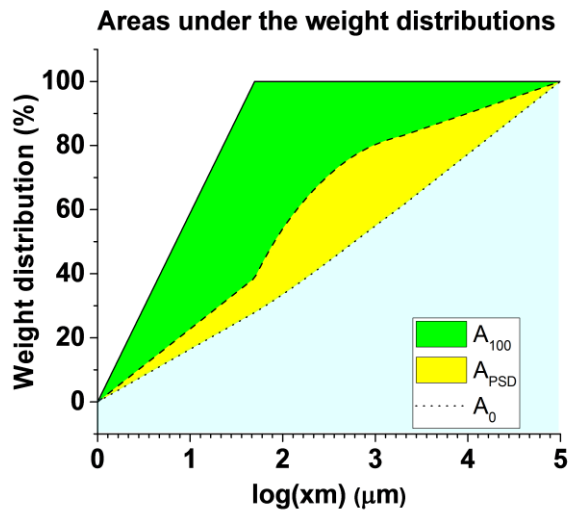
528 Figure 4.



529

530

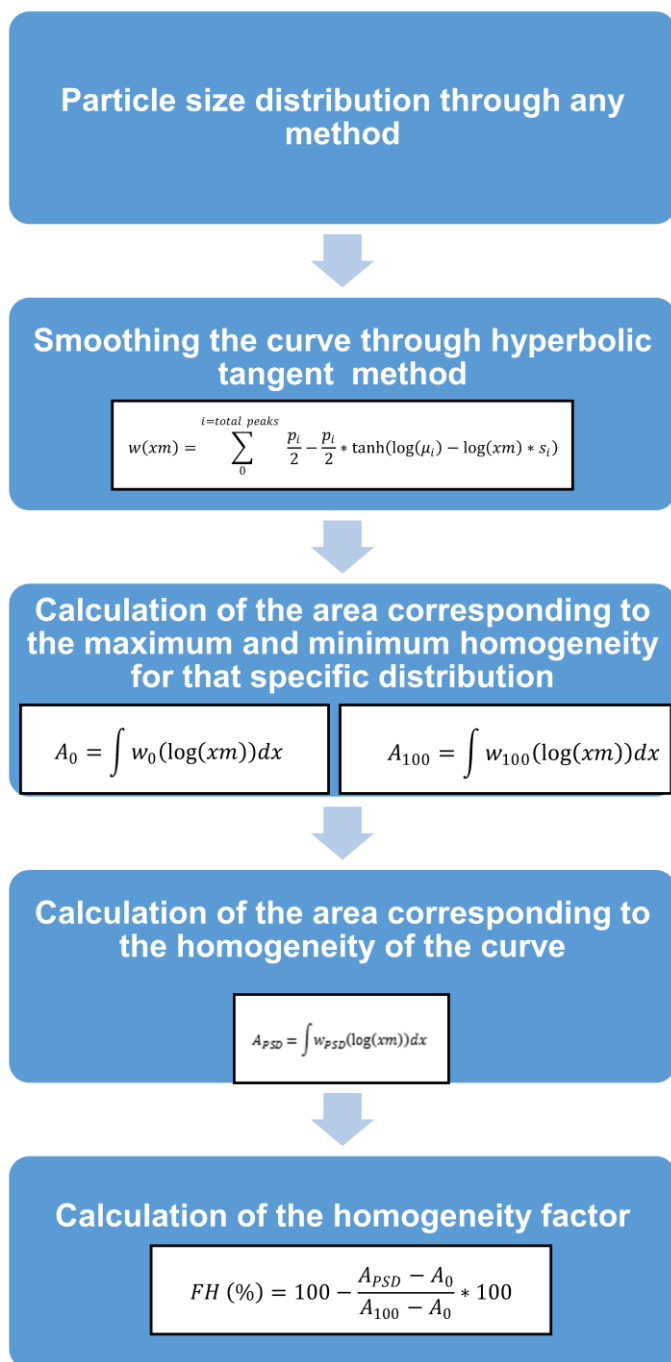
531 Figure 5.



532

533

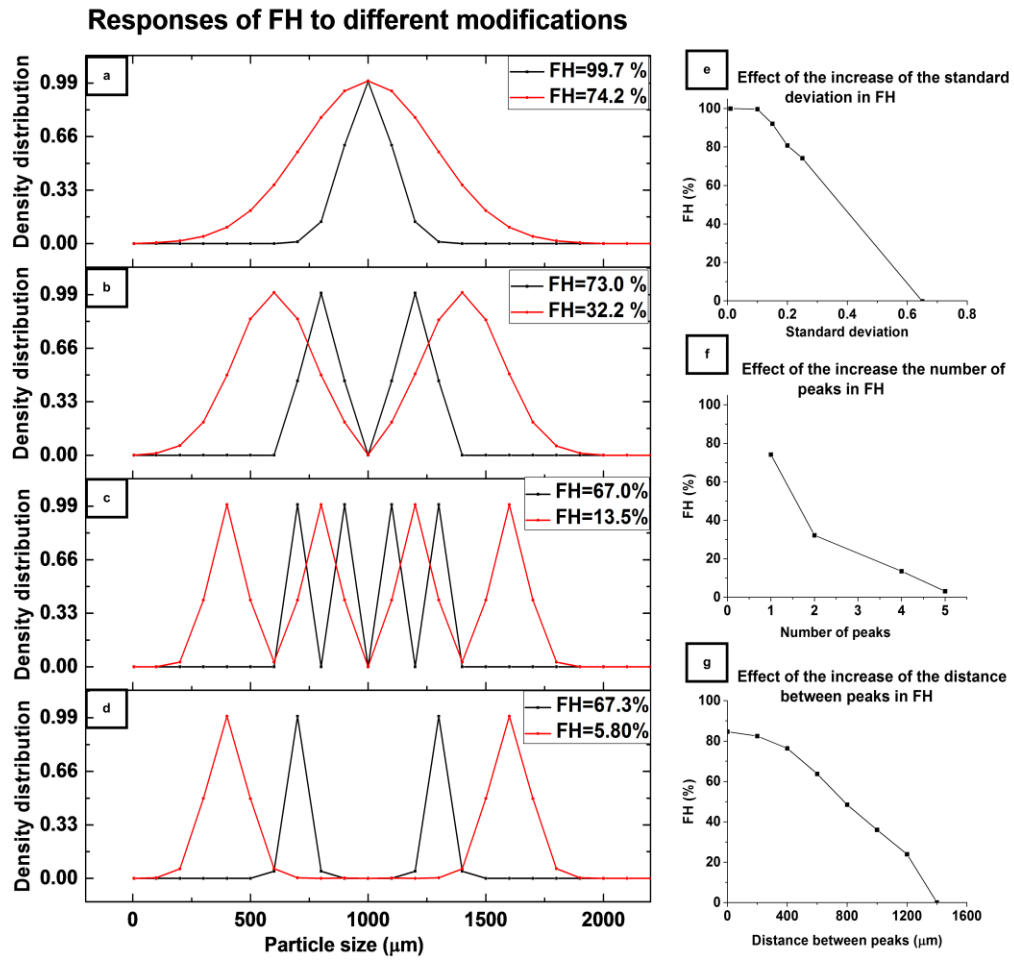
534 Figure 6.



535

536

537 Figure 7.

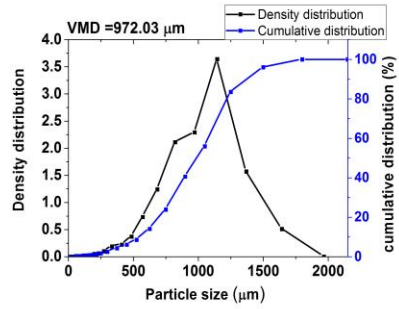
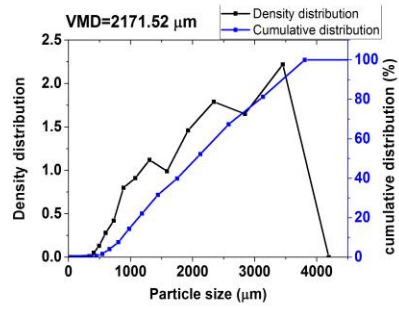
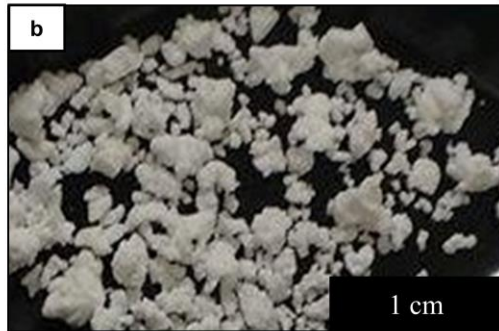
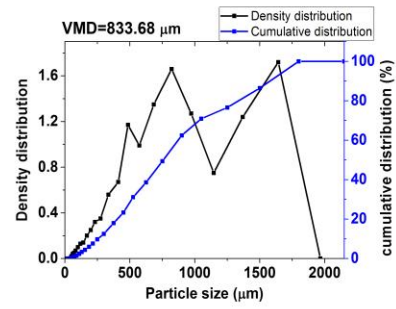


538

539

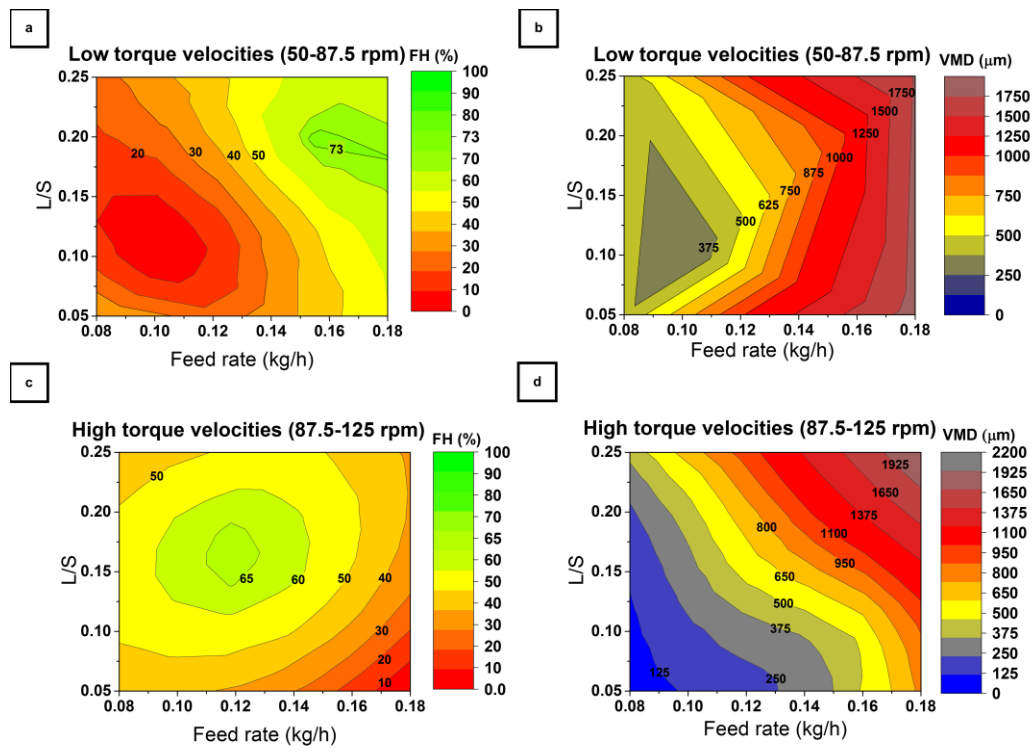
540 Figure 8.

541



542

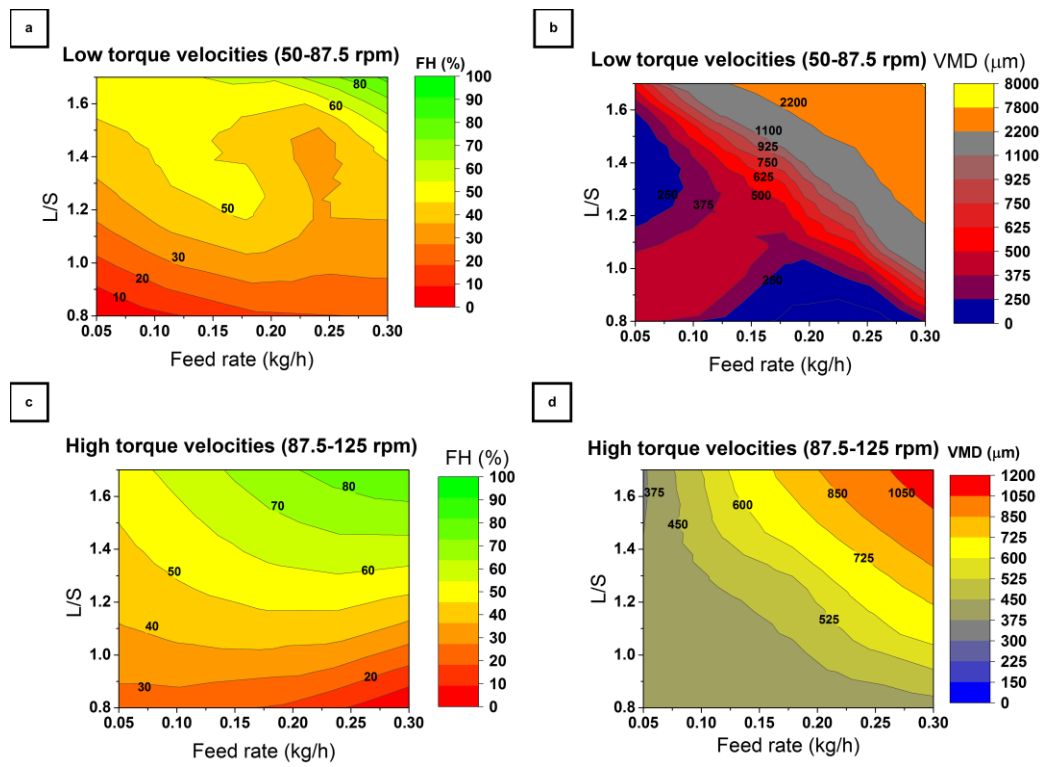
543 Figure 9.



544

545

546 Figure 10.



547

548